Synthesis, Structures, and the Cis–Trans Isomerization of Bis-Chelated Manganese Carbonyl Cations $Mn(CO)_2[PPh_2(CH_2)_2PPh_2]_2^+$

D. J. Kuchynka and J. K. Kochi*

Department of Chemistry, University of Houston, University Park, Houston, Texas 77204

Received June 13, 1988

The metastable carbonylmanganese(I) cation *cis*-$Mn(CO)_2(PPh_2CH_2CH_2PPh_2)_2^+$ is successfully isolated as a single crystal of the hexafluoroarsenate salt by stereospecific hydride abstraction from $HMn(CO)_2(DPPE)_2$ (I) with triphenylcarbenium ion. The rate of the thermal isomerization of *cis*-$Mn(CO)_2(DPPE)_2^+$ (*c*-II) to the trans cation (*t*-II) follows first-order kinetics with a half-life of ~10 h at room temperature. The oxidation of *cis*-$Mn(CO)_2(DPPE)_2^+$ to the dication *c*-III is found by fast-scan cyclic voltammetry (CV) to be chemically reversible. However, *c*-III spontaneously isomerizes to *trans*-$Mn(CO)_2(DPPE)_2^{2+}$ with a half-life of only a few milliseconds at 25 °C, as determined by quantitative CV analysis according to Feldberg's digital simulations. The facile cis–trans isomerization of $Mn(CO)_2(DPPE)_2^+$ is attributed to internal steric strain—particularly that induced by the nonbonded phenyl substituents as indicated by comparison of the cis and trans cation structures established by X-ray crystallography. *cis*-$Mn(CO)_2(DPPE)_2^+ AsF_6^-$ crystallized in the monoclinic *Cc* space group with lattice constants a = 13.244 (4), b = 19.721 (6), and c = 22.212 (7) Å, β = 97.62 (2)°, and Z = 4. *trans*-$Mn(CO)_2(DPPE)_2^+AsF_6^-$ crystallized in the triclinic $P\bar{1}$ space group with lattice constants a = 11.261 (5), 13.056 (4), and c = 20.100 (6) Å, α = 77.41 (2), β = 87.53 (3), and γ = 65.60 (2)°, and Z = 2.

The ligand substitution of metal carbonyls $M(CO)_6$ with 2 mol of a chelating diphosphine affords cis and/or trans isomers of $M(CO)_2[PPh_2(CH_2)_nPPh_2]_2$ with n = 1, 2, or 3. In terms of purely electronic effects on the thermodynamic stability, the cis isomer of bis(η^2-diphosphine) complexes of d^6 metal centers are calculated to be preferred over the trans isomer, although the energy difference between them is small.[1] The preference for the cis geometry derives from the trans influence that minimizes the better π-accepting CO ligands from sharing the same metal d orbitals.[2] Experimentally, the cis isomers are indeed formed under thermodynamic conditions (i.e., high-temperature reflux) from $M(CO)_2(PPh_2CH_2PPh_2)_2$ with Cr, Mo, and W,[3] $M(CO)_2(PPh_2CH_2CH_2PPh_2)_2$ with Mo and W,[4,5] and $M(CO)_2(PPh_2CH_2CH_2CH_2PPh_2)_2$ with Mo.[6] The isolation of the corresponding trans isomers requires indirect and elaborate preparative procedures, since they undergo thermal isomerization.[7-9] There are however exceptions, as in the formation of *trans*-$M(CO)_2(PPh_2CH_2CH_2PPh_2)_2$ as the favored isomer with M = Cr^0 and Mn^I when they are prepared under the conditions described above.[10-12] Such a reversal for the theoretically favored formation of the cis geometry is apparently unique to $PPh_2CH_2CH_2PPh_2$ (DPPE) insofar as the first-row transition metals Cr^0 and Mn^I are concerned (vide supra). In order to focus on this problem, we decided to synthesize the thermodynamically less favored *cis*-carbonylmanganese cation $Mn(CO)_2(DPPE)_2^+$ and to compare its molecular structure with that of the trans isomer by single-crystal X-ray crystallography. The kinetics of the thermally and oxidatively induced cis–trans isomerization of $Mn(CO)_2(DPPE)_2^+$ are also the subject of this study.

Results

I. Preparation of *cis*- and *trans*-$Mn(CO)_2(DPPE)_2^+$ Salts. The heretofore unknown salts of *cis*-$Mn(CO)_2(DPPE)_2^+$ (*c*-II) were prepared in roughly 80% yields by hydride abstraction from the recently prepared hydrido complex[13] $HMn(CO)_2(DPPE)_2$ (I) with triphenylcarbenium ion according to the stoichiometry

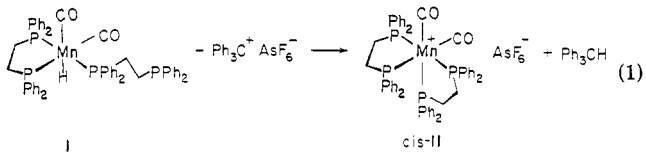

I cis-II (1)

The hydride replacement in eq 1 was facile, and it proceeded virtually to completion in dichloromethane within an hour at 0 °C. Thus the course of the hydride abstraction/ligand substitution in eq 1 could be readily followed by monitoring the monotonic decrease in the IR absorbance of the carbonyl stretching bands ν_{CO} = 1856 and 1915 cm^{-1} in I and the concomitant increase in the characteristic pair of bands at ν_{CO} = 1894 and 1950 cm^{-1} for *c*-II. The stereochemistry of the intramolecular route to the carbonylmanganese(I) cation in eq 1 follows from an intermolecular precedent by Berke and co-workers,[14] who isolated only *cis*-$Mn(CO)_2[P(OMe)_3]_4^+$ from the

(1) Marynick, D. S.; Askari, S.; Nickerson, D. F. *Inorg. Chem.* **1985**, *24*, 868.
(2) Burdett, J. K.; Albright, T. A. *Inorg. Chem.* **1979**, *18*, 2112.
(3) (a) Bond, A. M.; Colton, R.; Jackowski, J. J. *Inorg. Chem.* **1975**, *14*, 274. (b) Colton, R.; Howard, J. J. *Aust. J. Chem.* **1970**, *23*, 223.
(4) (a) Chatt, J.; Watson, H. R. *J. Chem. Soc.* **1961**, 4980. (b) Lewis, J.; Whyman, R. *J. Chem. Soc.* **1965**, 5486. (c) Reimann, R. H.; Singleton, E. *J. Organomet. Chem.* **1971**, *32*, C44.
(5) (a) Crossing, P. F.; Snow, M. R. *J. Chem. Soc. A* **1971**, 610. (b) Zingales, F.; Canziani, F. *Gazz. Chim. Ital.* **1962**, *92*, 343. (c) Sandhu, S. S.; Mehta, A. K. *J. Organomet. Chem.* **1974**, *77*, 45.
(6) (a) Bond, A. M.; Grabaric, B. S.; Jackowski, J. J. *Inorg. Chem.* **1978**, *17*, 2153. (b) Chow, T. J.; Wang, C.-Y.; Sheu, S.-C.; Peng, S.-M. *J. Organomet. Chem.* **1986**, *311*, 339.
(7) Bond, A. M.; Snow, M. R.; Wimmer, F. L. *Inorg. Chem.* **1974**, *13*, 1617. See also ref 3a and 6a.
(8) Datta, S.; McNeese, T. J.; Wreford, S. S. *Inorg. Chem.* **1977**, *16*, 2661 and Hanckel, J. M.; Darensbourg, M. Y. *J. Am. Chem. Soc.* **1983**, *105*, 6979.
(9) Holden, L. K.; Mawby, A. H.; Smith, D. C.; Whyman, R. *J. Organomet. Chem.* 1973, *55*, 343 and George, T. A.; Seibold, C. D. *Inorg. Chem.* **1973**, *12*, 2548.
(10) See ref 7 and the discussion therein.
(11) (a) Osborne, A. G.; Stiddard, M. H. B. *J. Chem. Soc.* **1965**, 700. (b) Sacco, A. *Gazz. Chim. Ital.* **1963**, *93*, 698.
(12) Kuchynka, D. J.; Kochi, J. K. *Inorg. Chem.* **1988**, in press.
(13) Kuchynka, D. J.; Kochi, J. K. *Inorg. Chem.*, in press.
(14) Berke, H.; Weiler, G. *Z. Naturforsch.* **1984**, *39B*, 431.

0276-7333/89/2308-0677$01.50/0

Table I. Data Collection and Processing Parameters for the X-ray Crystallography of $Mn(CO)_2(DPPE)_2^+$

	cis-$Mn(CO)_2$-$(DPPE)_2^+AsF_6^-$	*trans*-$Mn(CO)_2$-$(DPPE)_2^+AsF_6^-$
space group	*Cc*, monoclinic	$P\bar{1}$, triclinic
cell constants		
a, Å	13.244 (4)	11.261 (5)
b, Å	19.721 (6)	13.056 (4)
c, Å	22.212 (7)	20.100 (6)
α, deg		77.41 (2)
β, deg	97.62 (2)	87.53 (3)
γ, deg		65.60 (2)
V, Å^3	5750	2623
mol formula	$C_{54}H_{48}O_2P_4Mn^+ \cdot AsF_6^- \cdot 3C_2H_3N$	$C_{54}H_{48}O_2P_4Mn^+ \cdot AsF_6^- \cdot C_2H_3N$
fw	1219.9	1137.8
formula units per cell, *Z*	4	2
density, ρ, g cm^{-3}	1.41	1.44
abs coeff, μ, cm^{-1}	9.62	10.5
radiation (Mo Kα), λ, Å	0.710 73	0.710 73
collectn range, deg	$4 < 2\theta < 50$	$4 < 2\theta < 42$
scan width, deg	$\Delta\theta = 1.2 + (K\alpha_2 - K\alpha_1)$	$\Delta\theta = 1.2 + (K\alpha_2 - K\alpha_1)$
scan speed range, deg·min^{-1}	3.0–15.0	3.0–15.0
total data collected, $h + k = 2n$	5288	5639
independent data, $I > 3\sigma(I)$	4815	4504
total variables	407	376
$R = \sum\|\|F_o\| - \|F_c\|\|/\sum\|F_o\|$	0.045	0.058
$R_w = [\sum w(\|F_o\| - \|F_c\|)^2/\sum w\|F_o\|^2]^{1/2}$	0.034	0.048
weights	$w = \sigma(F)^{-2}$	$w = \sigma(F)^{-2}$

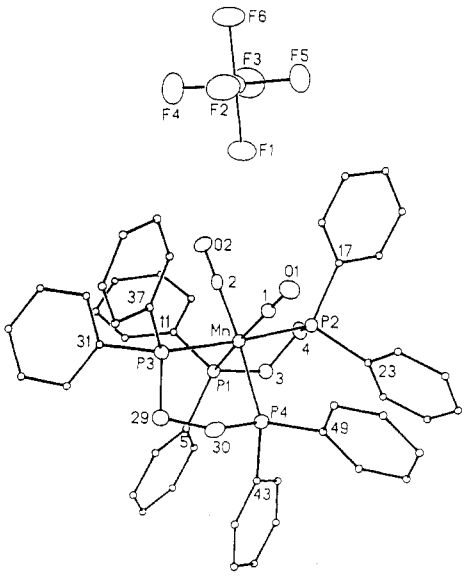

Figure 1. ORTEP diagram of *cis*-$Mn(CO)_2(DPPE)_2^+AsF_6^-$ showing the close nonbonded ion-pair interactions arising from the molecular cleft.

treatment of *cis*-$HMn(CO)_2[P(OMe)_3]_3$ with Ph_3C^+ in the presence of added trimethyl phosphite. They thus established that the ligand replacement of a neutral hydridomanganese(I) carbonyl via hydride abstraction proceeds with stereochemical retention.[15] The *cis*-$Mn(CO)_2$-$(DPPE)_2^+AsF_6^-$ was isolated as a bright yellow salt by column chromatography on neutral alumina at 0 °C.

(15) This process is reminiscent of the proton transfer from the seven-coordinate hydridomolybdenum cation *trans*-$HMo(CO)_2(DPPE)_2^+$ to afford the neutral *trans*-$Mo(CO)_2(DPPE)_2$.[8]

Table II. Selected Bond Angles (deg) in Carbonylmanganese(I) Cations

	cis-$Mn(CO)_2(DPPE)_2^+$		
P(2)–Mn–P(1)	83.6 (1)	P(3)–Mn–P(1)	99.4 (1)
P(3)–Mn–P(2)	176.0 (1)	P(4)–Mn–P(1)	100.6 (1)
P(4)–Mn–P(2)	99.0 (1)	P(4)–Mn–P(3)	83.1 (1)
C(1)–Mn–P(1)	169.3 (2)	C(1)–Mn–P(2)	86.3 (2)
C(1)–Mn–P(3)	90.5 (2)	C(1)–Mn–P(4)	84.4 (2)
C(2)–Mn–P(1)	84.8 (2)	C(2)–Mn–P(2)	88.6 (2)
C(2)–Mn–P(3)	89.0 (2)	C(2)–Mn–P(4)	171.1 (2)
C(2)–Mn–C(1)	91.5 (3)	C(3)–P(1)–Mn	107.5 (2)
O(1)–C(1)–Mn	176.8 (6)	O(2)–C(2)–Mn	179.1 (6)
C(4)–C(3)–P(1)	111.0 (4)	C(3)–C(4)–P(2)	111.8 (5)
C(6)–C(5)–P(1)	120.3 (5)	C(10)–C(5)–P(1)	119.8 (5)
	trans-$Mn(CO)_2(DPPE)_2^+$		
P(2)–Mn(1)P(1)	82.7 (1)	C(1)–Mn(1)–P(1)	93.0 (2)
C(1)–Mn(1)–P(2)	95.8 (2)	P(3)–Mn(2)–C(28′)	87.0 (2)
P(1)–Mn(1)–P(2′)	97.3 (1)	P(1)–Mn(1)–C(1′)	87.0 (2)
P(2)–Mn(1)–P(2′)	180.0	P(2)–Mn(1)–C(1′)	84.2 (2)
C(1)–Mn(1)–C(1′)	180.0	P(4)–Mn(2)–P(3)	82.9 (1)
C(28)–Mn(2)–P(3)	93.0 (2)	C(28)–Mn(2)–P(4)	93.5 (2)
P(3)–Mn(2)–P(3′)	180.0	P(3)–Mn(2)–P(4′)	97.1 (1)
		P(4)–Mn(2)–C(28′)	86.5 (2)
		C(3)–P(2)–Mn(1)	108.8 (2)
		O(2)–C(28)–Mn(2)	177.3 (6)

Table III. Selected Bond Distances (Å) in Carbonylmanganese(I) Cations

	cis-$Mn(CO)_2(DPPE)_2^+$		
Mn–P(1)	2.423 (2)	Mn–P(2)	2.304 (2)
Mn–P(3)	2.344 (2)	Mn–P(4)	2.411 (2)
Mn–C(1)	1.782 (6)	Mn–C(2)	1.772 (7)
P(1)–C(3)	1.835 (6)	P(1)–C(5)	1.834 (6)
P(1)–C(11)	1.831 (7)	P(2)–C(4)	1.830 (6)
P(2)–C(17)	1.835 (7)	P(2)–C(23)	1.843 (6)
P(3)–C(29)	1.831 (6)	P(3)–C(31)	1.835 (6)
P(3)–C(37)	1.854 (6)	P(4)–C(30)	1.838 (7)
P(4)–C(43)	1.830 (6)	P(4)–C(49)	1.839 (7)
O(1)–C(1)	1.154 (7)	O(2)–C(2)	1.168 (7)
C(3)–C(4)	1.528 (8)	C(5)–C(6)	1.388 (8)
	trans-$Mn(CO)_2(DPPE)_2^+$		
Mn(1)–P(1)	2.317 (2)	Mn(1)–P(2)	2.351 (2)
Mn(1)–C(1)	1.825 (8)	Mn(2)–P(3)	2.321 (2)
Mn(2)–P(4)	2.343 (2)	Mn(2)–C(28)	1.813 (9)
P(1)–C(2)	1.832 (9)	P(1)–C(4)	1.835 (6)
P(1)–C(10)	1.838 (7)	P(2)–C(3)	1.853 (7)
P(2)–C(16)	1.823 (6)	P(2)–C(22)	1.834 (9)
P(3)–C(29)	1.840 (7)	P(3)–C(31)	1.826 (8)
P(3)–C(37)	1.833 (6)	P(4)–C(30)	1.852 (8)
P(4)–C(43)	1.828 (6)	P(4)–C(49)	1.843 (9)
O(1)–C(1)	1.151 (10)	O(2)–C(28)	1.159 (10)
C(2)–C(3)	1.533 (8)	C(4)–C(5)	1.383 (9)

The trans isomer of $Mn(CO)_2(DPPE)_2^+$ was prepared by the direct, thermal ligand substitution of dimanganese decacarbonyl with 2 mol of DPPE according to eq 2.[12]

$$Mn_2(CO)_{10} + 2DPPE \rightarrow t\text{-}Mn(CO)_2(DPPE)_2^+Mn(CO)_5^- + 3CO \quad (2)$$

The mixed-salt *t*-$II^+Mn(CO)_5^-$ was collected as yellow-orange crystals in 75% yield and subsequently metathesized with ferrocenium hexafluorophosphate to yield *trans*-$Mn(CO)_2(DPPE)_2^+PF_6^-$ showing a single carbonyl IR band at 1897 cm^{-1}.[11,16]

II. Molecular Structures of *cis*- and *trans*-$Mn(CO)_2(DPPE)_2^+$. Single crystals of *cis*-$Mn(CO)_2$-$(DPPE)_2^+AsF_6^-$ suitable for X-ray crystallography were obtained by the slow diffusion of diethyl ether vapors into a concentrated acetonitrile solution for 24 h at 3 °C. The crystal data for *c*-II are listed in Table I together with other information pertinent to the X-ray crystallographic data

(16) Stiddard, M. H. B.; Snow, M. R. *J. Chem. Soc. A* **1966**, 777.

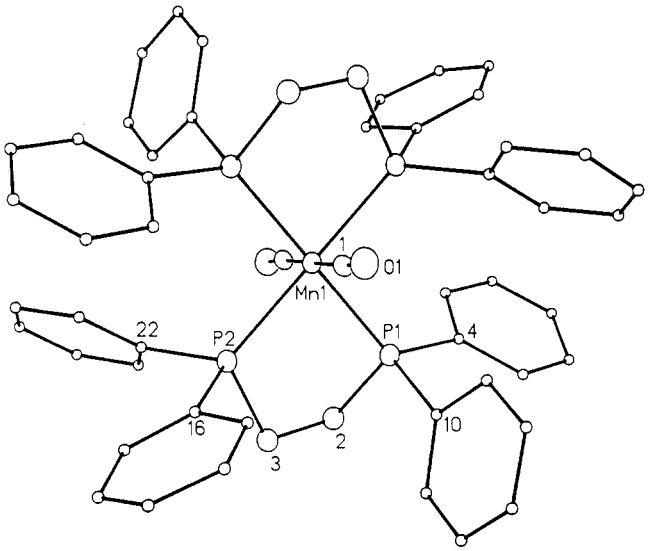

Figure 2. ORTEP diagram of *trans*-$Mn(CO)_2(DPPE)_2^+$ showing square-planar arrangement of phosphines in the equatorial plane.

collection and refinement. The ORTEP diagram in Figure 1 shows the pair of CO ligands in *c*-II to occupy nearly ideal cis positions around the octahedral manganese center, as described by the bond angles listed in Table II. The trans influence of the carbonyl ligands are shown by the pair of opposed Mn–P distances of 2.41 Å that are ~0.1 Å longer than those in which the phosphorus atoms are mutually trans (Table III). The two ethano bridges in the two DPPE ligands have torsion angles that are opposite in sign. As a result, there can be no twofold axis passing through manganese and bisecting the angle between the carbonyls as required by the space group $C2/c$. However we made no attempt to determine the sense of direction in this polar, nonenantiomorphous space group. Figure 1 also includes the hexafluoroarsenate counteranion that is strategically poised over the pair of cis carbonyl ligands—the center-to-center distance from manganese to arsenic being only 6.5 Å. Such a location corresponds to a cleft in the gross morphology of the *cis*-dicarbonylmanganese(I) cation to optimize the ion-pair interaction. Indeed such a tight ion pair may account for the very low solubility of *c*-II in tetrahydrofuran, certainly by comparison with that of the trans isomer.

Since no convenient procedure was available for the preparation of the corresponding trans salt of $Mn(CO)_2(DPPE)_2^+AsF_6^-$, a single crystal of its was prepared directly via the in situ isomerization of *cis*-$Mn(CO)_2(DPPE)_2^+AsF_6^-$ during the slow diffusion of diethyl ether vapors into an acetonitrile solution at *room temperature*. The crystal data for the bright orange *t*-II are also included in Table I. The ORTEP diagram shown in Figure 2 represents the average of two independent molecules of *trans*-$Mn(CO)_2(DPPE)_2^+$ found in the unit cell. Both molecules contained inversion centers but differed in the slight degree to which the phenyl rings in the coordinated DPPE ligands were twisted (see Experimental Section). The pair of trans carbonyl ligands in *t*-II occupy ideal trans positions around the octahedral manganese(I) center (see Table II). The Mn–CO distances of 1.81 Å are approximately 0.03 Å ($\sim 3\sigma$) shorter than those in the cis isomer (Table III). Such a difference can be attributed to the carbonyl trans influence (vide supra), and it is supported by lengths of 2.33 Å in all four Mn–P bonds. The hexafluoroarsenate counteranion is not shown in Figure 2 since it was found to bear no special relationship to the cation. This situation is thus in strong contrast with the highly ordered ion pair

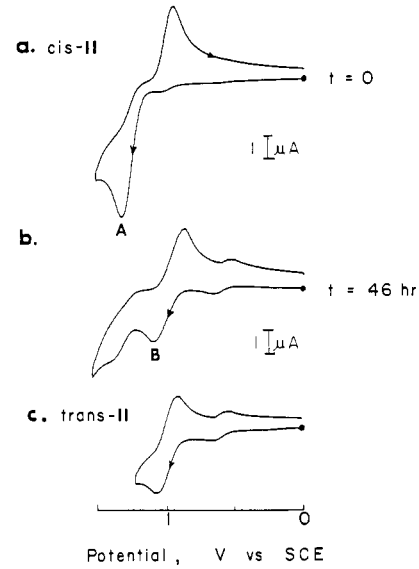

Figure 3. Initial positive-scan cyclic voltammograms at 23 °C of 5×10^{-3} M *cis*-$Mn(CO)_2(DPPE)_2^+AsF_6^-$ in tetrahydrofuran containing 0.3 M TBAP at $v = 0.5$ V s^{-1} (a) immediately upon dissolution and (b) 46 h later, compared to (c) 5×10^{-3} M *trans*-$Mn(CO)_2DPPE^+AsF_6^-$ under the same conditions.

found in *c*-II (vide supra). The average center-to-center distance of 7.5 Å from manganese to arsenic is also ~1 Å longer in the *t*-II salt, and it thus suggests a significantly reduced ion-pairing interaction compared to the *c*-II salt.

III. Thermal Rearrangement of *cis*-$Mn(CO)_2(DPPE)_2^+$. The orange solutions of *trans*-$Mn(CO)_2(DPPE)_2^+$ in acetonitrile were unchanged over prolonged periods, as judged by the persistence of the single, sharp carbonyl stretching band at the characteristic $\nu_{CO} = 1897$ cm^{-1}. The cis isomer *c*-II could also be formed in high yield (eq 1) and isolated as a pure crystalline salt. However the bright yellow solutions of *c*-II in acetonitrile on standing slowly darkened to orange, and inspection of the IR spectrum indicated the disappearance of the characteristic carbonyl stretching band at $\nu_{CO} = 1950$ cm^{-1} and concomitant growth of the band at $\nu_{CO} = 1897$ cm^{-1} of the trans isomer, i.e., eq 3. Since the carbonyl band at 1897 cm^{-1}

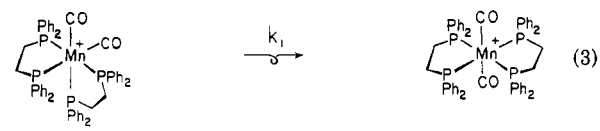

(3)

could not be quantitatively resolved from the low-energy band of *c*-II at $\nu_{CO} = 1894$ cm^{-1}, the appearance of *trans*-$Mn(CO)_2(DPPE)_2^+$ could not be successfully monitored by IR analysis. However, the isomerization of *cis*-$Mn(CO)_2(DPPE)_2^+$ was also apparent in the time-dependent cyclic voltammograms (CV) in tetrahydrofuran solutions containing 0.1 M tetrabutylammonium perchlorate (TBAP). Thus the initial positive-scan CV of *c*-II in Figure 3a shows an irreversible anodic wave A with a peak potential $E_a = 1.30$ V vs SCE at a scan rate $v = 500$ mV s^{-1}. This solution on standing yielded a reversible cyclic voltammogram (Figure 3b) in which the anodic peak potential had undergone a negative shift to the anodic wave B at $E_a = 1.07$ V. Indeed the latter corresponded to the cyclic voltammogram of *trans*-$Mn(CO)_2(DPPE)_2^+$, as also established by comparison with that of authentic *t*-II in Figure 3c. The reversible electrode process occurred at $E^0 = 0.88$ V vs SCE; and the cathodic/anodic peak current ratio i_c/i_a was unity with $\Delta E = 83$ mV at a scan rate of v

Table IV. Thermal Isomerization of *cis*-$Mn(CO)_2(DPPE)_2^+$ [a]

solvent	additive	$10^5 k_1$, s^{-1}	method
dichloromethane	none	2.0	IR[b]
acetonitrile	none	1.5	IR[b]
tetrahydrofuran	TBAP[c]	1.0[d]	CV
		1.0[e]	CV
dichloromethane	CO[f]	3.2	IR[b]
dichloromethane	DPPE[g]	2.3	IR[b]

[a] With 5×10^{-3} M *cis*-$Mn(CO)_2(DPPE)_2^+AsF_6^-$ at 23 °C. Reproducibility ±10%. [b] By disappearance of characteristic carbonyl band at 1950 cm^{-1}. [c] 0.3 M tetra-*n*-butylammonium perchlorate. [d] Disappearance of *c*-II by CV analysis of E^0 = 1.30 V. [e] Appearance of *t*-II by CV analysis of E_a = 1.07 V. [f] 1 atm carbon monoxide. [g] 5 equiv of added $PPh_2CH_2CH_2PPh_2$.

= 500 mV s^{-1}. The reversible CVs observed even at very high scan rates of $v \sim 10$ V s^{-1} indicated that electron transfer occurred with retention of configuration, i.e., eq 4. The well-behaved cyclic voltammogram of *trans*-$Mn(CO)_2(DPPE)_2^+$ allowed its concentration to be determined from the anodic peak current (i_a) at v = 500 mV s^{-1}.

$$t\text{-}Mn(CO)_2(DPPE)_2^+ \overset{-e}{\rightleftharpoons} t\text{-}Mn(CO)_2(DPPE)_2^{2+} \quad (4)$$

The kinetics of the cis to trans isomerization of $Mn(CO)_2(DPPE)_2^+$ was followed by two independent procedures. In the first method, the disappearance of *c*-II was followed by monitoring the decrease of the carbonyl band at 1950 cm^{-1}. The first-order plots of the absorbance change were linear to at least 4 half-lives with correlation coefficient $r > 0.99$. The first-order rate constants k_1 in eq 3 are listed in Table IV. The magnitude of k_1 in acetonitrile was essentially the same as that obtained in the less polar dichloromethane. Furthermore the presence of 5 equiv of added DPPE or an atmosphere of carbon monoxide effected little change in k_1. In the second method, the appearance of *trans*-$Mn(CO)_2(DPPE)_2^+$ was monitored by cyclic voltammetry at v = 500 mV s^{-1} in tetrahydrofuran solution containing 0.1 M tetrabutylammonium perchlorate. Under these conditions the anodic peak potentials of *c*-II and *t*-II at E_a = 1.30 and 1.08 V, respectively, were sufficiently well-resolved to allow quantitative analysis of the mixtures of cis/trans isomers. Both the disappearance of *cis*-$Mn(CO)_2(DPPE)_2^+$ and the appearance of the trans isomer monitored by this procedure followed first-order kinetics. The rate constants k_1 are also included in Table IV, and within the experimental uncertainties they are the same as those determined by IR analysis. The cis–trans isomerization in eq 3 was not complicated by side reactions, since no spurious peaks were noted in the course of either IR or CV analysis.

The cis–trans isomerization of $Mn(CO)_2(DPPE)_2^+$ was also observed in the solid state. For example, a pure crystal of *cis*-$Mn(CO)_2(DPPE)_2^+AsF_6^-$ contained in a screw-cap vial (with no precaution to remove air) underwent an approximately 40% conversion to the trans isomer when left for a week at room temperature. This solid-state conversion was presumably similar to that described by eq 3 for the homogeneous, solution process. It was not examined further.

IV. Oxidatively Induced Isomerization of *cis*-$Mn(CO)_2(DPPE)_2^+$. When a yellow solution of 5×10^{-3} *cis*-$Mn(CO)_2(DPPE)_2^+$ in acetonitrile containing 0.1 M TBAP was exhaustively oxidized at a controlled potential of E = 1.50 V, it turned dark blue green with an electron uptake of 1.0 ± 0.05 C/mol of the cation *c*-II charged. IR analysis of the anolyte indicated the complete disappearance of *c*-II with its twin carbonyl bands at ν_{CO} = 1894 and 1950 cm^{-1}, and the simultaneous appearance of a single new band at ν_{CO} = 1966 cm^{-1}. The latter was associated with a paramagnetic species with an isotropic ESR spectrum at $\langle g \rangle$ = 2.000 14 in Figure 4 showing a sextet splitting due to ^{55}Mn ($I = {}^5/_2$) with the hyperfine splitting of a_{Mn} = 95 G.[17] The species was readily assigned to the paramagnetic dication *trans*-$Mn(CO)_2(DPPE)_2^{2+}$, as also indicated by its reversible CV with $E°$ = 0.88 V that was observed upon an initial negative scan of the anolyte (compare eq 4). Thus in the course of anodic oxidation (approximately 30 min), the cis monocation *c*-II was completely converted to the trans dication *t*-III, i.e., eq 5. It is important to emphasize that the thermal rearrangement in eq 3 occurred much too slowly to participate in any significant way to the process in eq 5.

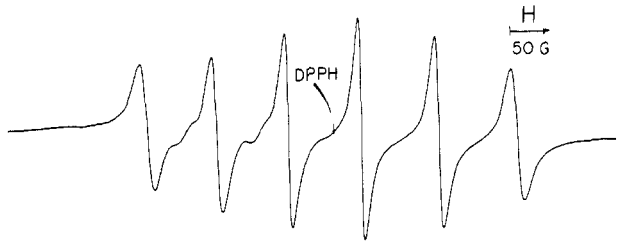

Figure 4. ESR spectrum of $Mn(CO)_2(DPPE)_2^{2+}$ (with DPPH field marker) formed from the anodic oxidation of either *cis*- or *trans*-$Mn(CO)_2(DPPE)_2^+$ in acetonitrile.

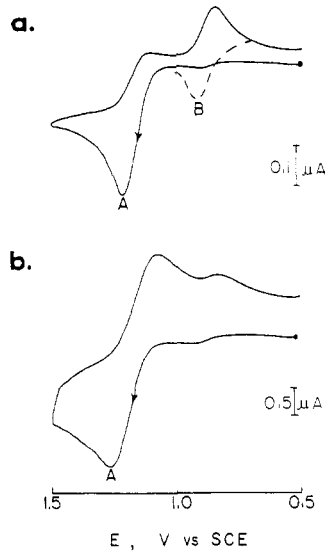

Figure 5. Initial positive-scan cyclic voltammogram at 0 °C of 5×10^{-3} M *cis*-$Mn(CO)_2(DPPE)_2^+$ in acetonitrile containing 0.1 M TBAP with a platinum electrode at (a) v = 2 V s^{-1} and (b) v = 100 V s^{-1}. Dashed curve shows the reversible anodic wave B on the return scan.

$$cis\text{-}Mn(CO)_2(DPPE)_2^+ \overset{-e}{\longrightarrow} trans\text{-}Mn(CO)_2(DPPE)_2^{2+} \quad (5)$$
$$\text{c-II} \qquad\qquad \text{t-III}$$

In order to ascertain the source of the rearrangement, we examined the cyclic voltammetry of *c*-II at 0 °C at several scan rates. The initial positive-scan cyclic voltammograms of *c*-II in acetonitrile containing 0.1 M TBAP at v = 2 and 100 V s^{-1} are shown in parts a and b, respectively, of Figure 5. Two features of these sweep-dependent CV's are noteworthy. First, the irreversible anodic wave A with E_a = 1.22 V in Figure 5a becomes chemically reversible with E^0 = 1.19 V at the higher scan rate shown

(17) The hyperfine splittings arising from ^{31}P could not be resolved within the experimental line widths of $\Delta H_{PP} \approx 11$ G.

Table V. Oxidatively Induced Isomerization of *cis*-$Mn(CO)_2(DPPE)_2^+$ [a]

temp, °C	first-order rate constant k_2,[b] s^{-1} working curve[c]	CV simulation[d]
0	21	23
23	103	120

[a] From 5×10^{-3} M *cis*-$Mn(CO)_2(DPPE)_2^+AsF_6^-$ in acetonitrile containing 0.1 M TBAP at 23 °C. [b] Reproducibility ±15%. [c] Derivation of Nicholson and Shain in ref 22. [d] Digital simulation of CV according to Feldberg in ref 23.

in Figure 5b. Such a CV behavior underscores the short lifetime of the cis dication *c*-III. Second, the cathodic wave B at $E_c = 0.84$ observed on sweep reversal in Figure 5a is associated with the trans dication *t*-III shown by the reversible CV couple (with the coupled anodic wave B indicated as a dashed curve) at $E^0 = 0.88$ V, as described in eq 4.[18] Since *t*-III appears only after the reversible oxidation of the cis cation *c*-II, it follows that it is formed by the spontaneous rearrangement of the metastable cis dication *c*-III. This facile cis–trans rearrangement of the dication $Mn(CO)_2(DPPE)_2^{2+}$ is included in the ECE mechanism in Scheme I. The overall transformation for

Scheme I

$$c\text{-II} \overset{-e}{\rightleftharpoons} c\text{-III} \quad (6)$$

$$c\text{-III} \xrightarrow[0]{k_2} t\text{-III} \quad (7)$$

$$t\text{-III} \overset{+e}{\rightleftharpoons} t\text{-II} \quad (8)$$

the ECE process in Scheme I corresponds to the isomerization of the cis monocation to the trans isomer *t*-II reminiscent of that in eq 3. However it differs from the relatively straightforward thermal process in eq 3 in that it proceeds via a prior electron transfer. As such, this cis–trans conversion of the carbonylmanganese cation II is designated as an *oxidatively induced rearrangement*. Two questions arise immediately. Is it a chain process similar to the electron transfer chain or ETC catalysis that is observed in other carbonylmetal rearrangements?[19] How fast does the dication isomerize in eq 7 in comparison with the monocation in eq 3?

When the bulk anodic oxidation of *c*-II was interrupted periodically and small aliquots of anolyte removed, IR or CV analysis indicated that the product *t*-III was always present in amounts corresponding to the fraction of charge (i.e., coulombs) passed through the solution. This result rules out any chain process such as the aforementioned ETC catalysis.[19,20] Accordingly we focussed on the stoichiometric pathway described in Scheme I to determine the rate constant for the rearrangement step in eq 7. Two analytic procedures were employed. In the first method, the cathodic/anodic current ratios i_c/i_a at various scan rates v were fitted to the working curves derived by Nicholson and Shain.[22] Although conveniently independent of the electrochemical kinetics, this method requires accurate (and difficult to measure) values of the current ratio, and it is thus difficult to apply quantitatively. Nonetheless the best values of k_2 for eq 7 obtained by this procedure

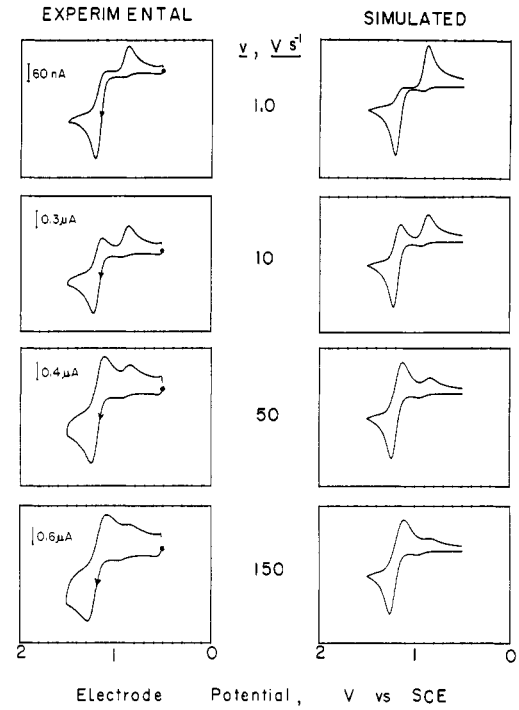

Figure 6. Comparison of the experimental (left) and computer-simulated (right) cyclic voltammograms at various scan rates (v) of *cis*-$Mn(CO)_2(DPPE)_2^+$ based on Feldberg's method. [Note the pronounced charging currents induced at high scan rates were not included in the CV simulations.]

Table VI. Electrochemical Kinetics Parameters for *cis*- and *trans*-$Mn(CO)_2(DPPE)_2^+$ [a]

redox couple	E^0, V vs SCE	α[b]	k_s,[b] cm s^{-1}	D,[c] cm^2 s^{-1}
cis-II/*cis*-III	1.19	0.4	0.052	*d*
trans-II/*trans*-III	0.88	0.5	0.047	8.6×10^{-6}

[a] Data from 5×10^{-3} M $Mn(CO)_2(DPPE)_2^+AsF_6^-$ in acetonitrile containing 0.1 M TBAP at a Pt electrode at 23 °C. [b] Method in ref 26. [c] Method in ref 27. [d] Taken to be the same as *trans*-II.

are listed in Table V at two temperatures. In the second method, we performed digital simulations of the cyclic voltammograms at various sweep rates using the finite difference approach of Feldberg.[23,24] Unlike the Nicholson and Shain analysis, the digital simulation of the cyclic voltammogram in Figure 6 requires a knowledge of the electrochemical parameters: the reversible potential E^0, the transfer coefficient α, and the heterogeneous rate constant k_s together with the diffusion coefficient D. Owing to the reversible nature of both couples, i.e., *c*-II $\rightleftharpoons$ *c*-III and *t*-II $\rightleftharpoons$ *t*-III, values of E^0, α, and k_s were determined by standard methods,[25-27] and they are tabulated in Table VI. The acceptable agreement in the values of k_2 in Table V determined by digital simulation with those based on the Nicholson and Shain working curves reinforces our confidence in the essential correctness of the mechanism in Scheme I.

Discussion

The cis and trans stereoisomers of the carbonylmanganese(I) cation $Mn(CO)_2(DPPE)_2^+$ can be viewed as

(18) Note the presence of the minor anodic wave at $E_a = 0.92$ V in the initial positive scan in Figure 5 was traced to small amounts of *t*-II as an impurity in the starting *cis*-$Mn(CO)_2(DPPE)_2^+AsF_6^-$.

(19) (a) Bond, A. M.; Colton, R.; McGregor, K. *Inorg. Chem.* **1986**, *25*, 2378. (b) Bond, A. M.; Colton, R.; Kevekordes, J. E. *Inorg. Chem.* **1986**, *25*, 749. (c) Bond, A. M.; Carr, S. W.; Colton, R. *Organometallics* **1984**, *3*, 541.

(20) Compare also some related ETC processes of carbonylmetals such as ligand substitution.[21]

(21) Kochi, J. K. *J. Organomet. Chem.* **1986**, *300*, 139.

(22) Nicholson, R. S.; Shain, I. *Anal. Chem.* **1964**, *36*, 706.

(23) Feldberg, S. W. In *Electroanalytical Chemistry*; Bard, A. J., Ed.; Marcel Dekker: New York, 1969; Vol. 3; pg 199.

(24) Feldberg, S. W. In *Computer Application in Analytical Chemistry*; Mark, H. B., Ed.; Marcel Dekker: New York, 1972; p 185.

(25) Bard, A. J.; Faulkner, L. R. *Electrochemical Methods*; Wiley: New York, 1980.

(26) Nadjo, L.; Saveant, J. M. *J. Electroanal. Chem.* **1973**, *48*, 113.

(27) Howell, J. O.; Wightman, R. M. *Anal. Chem.* **1984**, *56*, 524.

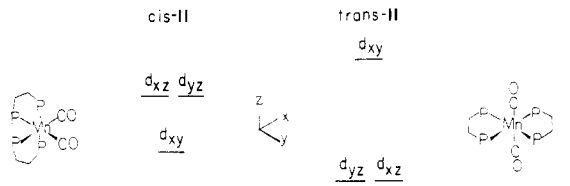

Figure 7. Relative ordering of HOMO energies of isomeric *cis*- and *trans*-$Mn(CO)_2P_4$ according to Bond and co-workers.[10]

different in two important ways—the trans cation *t*-II is the thermodynamically more stable isomer, but its HOMO energy (as indicated by the more negative value of the oxidation potential E^0) is higher than that of *cis*-$Mn(CO)_2(DPPE)_2^+$ (*c*-II).

I. Steric Differences in *cis*- and *trans*-$Mn(CO)_2(DPPE)_2^+$. The foregoing, apparently contradictory, conclusions can be reconciled if the differences in the internal steric strain of *cis*- and *trans*-$Mn(CO)_2(DPPE)_2^+$ are taken into consideration. For example, the visual inspection of the ORTEP diagram in Figure 1 for *cis*-$Mn(CO)_2(DPPE)_2^+$ reveals the presence of a pair of rather severe nonbonded or 1,3-phenyl interactions centered on the aromatic rings 23/49 and 11/31 in the pair of coordinated DPPE ligands. Such a steric congestion undoubtedly arises from the mutually cis orientation of the DPPE ligands that separates the more or less face-to-face phenyl rings by an average interannular distance of only ~3.3 Å. By way of contrast, the ORTEP diagram in Figure 2 for the trans isomer *t*-II shows a more open molecular structure, since the corresponding phenyl rings only suffer a roughly edge-to-face interaction. The relief of such unfavorable steric interactions (which exceed the difference in HOMO energies) in the cis cation would account for the experimentally observed cis–trans isomerization of $Mn(CO)_2(DPPE)_2^+$. This qualitative explanation also accords with the observation that the cis and trans isomers of the isoelectronic $Cr(CO)_2(DPPE)_2$ are *both* formed during ligand substitution of $Cr(CO)_6$ with DPPE in refluxing decane solution.[7,28] Thus the longer covalent bond radius of the neutral chromium(0) complex would lead to a lower steric strain and to a smaller driving force for cis–trans isomerization in comparison with those extant in the cationic manganese(I) analogues. Whether steric compression is always the determining factor is not apparent in the observation that the methyl derivative $Cr(CO)_2(PMe_2CH_2CH_2PMe_2)_2$ is known to be cis.[29] Although this chelating ligand has more or less the same bite angle as DPPE,[30,31] the increased trans influence by the alkyl- rather than arylphosphine center as the σ-donor could be the determining factor.[34] Thus the generalized energy ordering of the filled t_{2g} molecular orbitals of the cis and trans isomers of $Mn(CO)_2P_4$ complexes by Bond and coworkers[10] in Figure 7 is qualitatively consistent with the molecular structures and redox properties of $Mn(CO)_2(DPPE)_2^+$, as established in this study. Important to their formulation is the raising of the HOMO energies of the trans isomer resulting from the better σ-donor properties of phosphine (P) relative to CO and the converse order of ligand π-acidities.

II. Thermal Isomerization of *cis*-$Mn(CO)_2(DPPE)_2^+$. The magnitude of the steric strain in *cis*-$Mn(CO)_2(DPPE)_2^+$ is not so large, as evidenced by the rather slow rates of conversion to the trans cation *t*-II (Table IV). Moreover the first-order kinetics that are largely unaffected by solvent polarity and by added DPPE or excess CO pressure point to a unimolecular pathway for cis–trans isomerization.

There is a growing body of evidence for the twist mechanism[35] for cis–trans isomerization in octahedral metal complexes, although the activation barrier is predicted to be quite high.[36-40] For example, the isomerization of the metastable *trans*-$M(CO)_2(DPPE)_2$ with M = Mo and W[7-9] has been considered to be an intramolecular process based on rates that are insensitive to solvent effects as well as to added ligands (DPPE and CO), and they have large, negative entropies of activation.[6,8,41] However with bidentate phosphine ligands such as DPPE, care must be exercised in formulating an intramolecular twist mechanism for first-order processes, since a prior ligand dissociation to yield a coordinatively unsaturated η^1-diphosphine intermediate followed by isomerization and religation is kinetically difficult to rule out.[42,43]

III. Oxidatively Induced Isomerization of *cis*-$Mn(CO)_2(DPPE)_2^+$. Cis-trans isomerization is enhanced markedly by the oxidative conversion of *cis*-$Mn(CO)_2(DPPE)_2^+$ to its dication. Thus the magnitude of the first-order rate constant k_1 in Table IV increases by 7 orders of magnitude for k_2 in Table V. Such a large rate enhancement may derive partly from a larger driving force for cis–trans isomerization in $Mn(CO)_2(DPPE)_2^{2+}$ resulting from a steric contraction of the dication.[44] Unfortunately, the dication *cis*-$Mn(CO)_2(DPPE)_2^{2+}$ is too transient to allow isolation of its salt for crystallographic analysis to establish this point. Nonetheless we are more inclined to attribute the enhanced rates to a lowering of the activation barrier for cis–trans isomerization of $Mn(CO)_2(DPPE)_2^{2+}$. For example from the qualitative splitting of the t_{2g} levels in Figure 7 according to Bond and co-workers,[10] the oxidation of *trans*-$Mn(CO)_2(DPPE)_2^+$ removes an electron from a higher lying d_{xy} orbital of the trans product and leaves the low-lying, degenerate d_{xz}/d_{yz} pair filled.[34] The extent to which the transition state takes on productlike

(28) The actual isomer distribution of cis and trans isomers formed in the preparation of $Cr(CO)_2(DPPE)_2$ or their interconversion has not been reported. The fact that *cis*-$Cr(CO)_2(DPPE)_2$ but no *cis*-$Mn(CO)_2(DPPE)_2^+$ is formed during ligand substitution provides only a qualitative indication of thermodynamic differences.

(29) Salt, J. E.; Girolami, G. S.; Wilkinson, G.; Motevalli, M.; Thornton-Pett, M.; Hursthouse, M. B. *J. Chem. Soc., Dalton Trans.* **1985**, 685.

(30) The effect of bite angle is seen on the very stable *cis*-$Cr(CO)_2(PPh_2CH_2PPh_2)_2$.[3]

(31) Defined as the P_1–M–P_2 angle, where P_1 and P_2 are the opposite ends of a chelating diphosphine. For $Ph_2P(CH_2)_nPPh_2$, the following bite angles are observed: DPPM (n = 1) ≅ 63.5°;[32] DPPE (n = 2) ≅ 80°;[33] DPPP (n = 3) ≅ 86°.[69]

(32) Drew, M. G. B.; Wolters, A. P.; Tomkins, I. B. *J. Chem. Soc., Dalton Trans.* **1977**, 974.

(33) This work and ref 8.

(34) Internal strain imposed by steric interactions of phenyl groups in the cis isomer was considered by Bond et al.[10] to lead to a decrease in ligand field strength.

(35) Cotton, F. A.; Wilkinson, G. In *Advanced Inorganic Chemistry*, Wiley: New York, 1980; p 1220.

(36) (a) Muetterties, E. L. *J. Am. Chem. Soc.* **1968**, *90*, 5097. (b) Muetterties, E. L. *Acc. Chem. Res.* **1970**, *3*, 266. (c) Albright, T. A., personal communication.

(37) (a) Pomeroy, R. K.; Graham, W. A. G. *J. Am. Chem. Soc.* **1972**, *94*, 274. (b) Fischer, E. O.; Fischer, H. *Chem. Ber.* **1974**, *107*, 657. (c) Dombek, B. D.; Angelici, R. J. *J. Am. Chem. Soc.* **1976**, *98*, 4110.

(38) (a) Darensbourg, D. J.; Cotton, F. A.; Klein, S.; Kolthammer, B. W. S. *Inorg. Chem.* **1982**, *21*, 2661. (b) Darensbourg, D. J.; Baldwin, B. J. *J. Am. Chem. Soc.* **1979**, *101*, 6447. (c) Darensbourg, D. J. *Inorg. Chem.* **1979**, *18*, 14.

(39) (a) Fischer, H. F.; Fischer, E. O.; Werner, H. *Angew. Chem., Int. Ed. Engl.* **1972**, *11*, 644. (b) Fisher, H. F.; Fischer, E. O.; Werner, H. *J. Organomet. Chem.* **1974**, *73*, 331.

(40) (a) Darensbourg, D. J.; Gray, R. L. *Inorg. Chem.* **1984**, *23*, 2993. (b) Ismail, A. A.; Sauriol, F.; Sedman, J.; Butler, I. S. *Organometallics* **1985**, *4*, 1914.

(41) Elson, C. M. *Inorg. Chem.* **1976**, *15*, 469.

(42) Compare Dobson, G. R.; Rettenmaier, A. J. *Inorg. Chim. Acta.* **1972**, *6*, 507.

(43) Brown, T. L.; Cohen, M. A. *Inorg. Chem.* **1976**, *15*, 1417.

(44) Douglas, B.; McDaniel, D. H.; Alexander, J. H. *Concepts and Models of Inorganic Chemistry*, 2nd ed.; Wiley: New York, 1983.

character would result in the lowering of the activation barrier for cis–trans isomerization. Indeed, the facile rearrangement of a variety of other 17e carbonylmetal complexes has been demonstrated, mainly by the pioneering work of Bond, Connelly, and co-workers.[45,46] For the d^6 complexes *cis*-$M(CO)_2(P\frown P)_2$ with M = Cr, Mo, or W and $P\frown P = PPh_2(CH_2)_{1,2,3}PPh_2$, the oxidation results in 17e trans cations that are isolable.[7] The rates of isomerization increase in the order Cr < Mo < W with half-lives of about 20 ms.[6a,41,47] Such rearrangements were also proposed to proceed via intramolecular pathways. The roughly fourfold faster rates observed with *cis*-$Mn(CO)_2(DPPE)_2^{2+}$ relative to the group VI carbonylmetals may reflect the increased orbital splitting owing to the cationic character of both the 18e and 17e carbonylmanganese species. Further studies of solvent variation and effects of additives could reveal deeper mechanistic insight into the latter.

Experimental Section

Materials. Manganese decacarbonyl (Pressure Chemical Co.) and triphenylmethyl hexafluoroarsenate (Ozark-Mahoning) were used as received. Bis(1,2-diphenylphosphino)ethane (DPPE; Pressure Chemical Co.) was recrystallized from absolute ethanol and dried in vacuo. Tetra-*n*-butylammonium perchlorate (TBAP; Pfaltz and Bauer) was recrystallized three times from a mixture of ethyl acetate and hexane, dried in vacuo, and stored in a desiccator over P_2O_5. Tetrahydrofuran (Fisher Scientific) was stirred with $LiAlH_4$ for 24 h and fractionally distilled under an argon atmosphere, and the distillate was stored in Schlenk flasks (with teflon stopcocks) under an argon atmosphere. Acetonitrile (Fisher analytical reagent) was stirred with $KMnO_4$ for 24 h at 25 °C and then heated at reflux until the precipitation of MnO_2 was complete. After removal of the brown solid by decantation, the solution was treated with P_2O_5 and a small amount of diethylenetriamine and the mixture refluxed for 5 h. Fractionation under an argon atmosphere was followed by treatment with CaH_2 and a second fractionation under an argon atmosphere to yield anhydrous acetonitrile which was stored in Schlenk flasks. Dichloromethane (Fisher, analytical reagent) was stirred with successive portions of 98% sulfuric acid until the acid layer was colorless. The resulting dichloromethane was washed with 5% aqueous $NaHCO_3$ and water. After the solution was dried over $CaCl_2$, the dichloromethane was refluxed with P_2O_5 and fractionated under an argon atmosphere. This pure, dry dichloromethane was subjected to a second fractionation over CaH_2 and the distillate stored in a Schlenk flask under an argon atmosphere. The last step ensured the production of acid-free dichloromethane, since traces of acid are known to catalyze the isomerization of metal carbonyls.[48]

Instrumentation. Infrared spectra were recorded with 0.1-mm NaCl cells on a Nicolet 10DX FT spectrometer. The ^1H and ^{31}P NMR spectra were obtained on a JEOL FX90Q or Nicolet NT300-WB spectrometer, and chemical shifts are reported relative to TMS and H_3PO_4, respectively. ESR spectra were recorded on a Varian E110 spectrometer using a DPPH lock. The conventional cyclic voltammetry at scan rate $v < 100$ V s^{-1}, preparative-scale electrolysis, and fast-scan cyclic voltammetry at $v > 200$ V s^{-1} were described previously.[12,49]

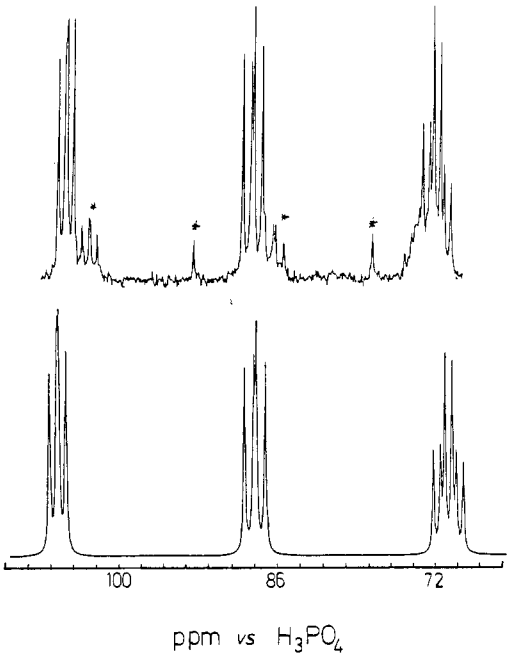

Figure 8. Upper: $^{31}P\{^1H\}$ NMR spectrum of $HMn(CO)_2(DPPE)_2$ in $CDCl_3$ at −60 °C. Lower: computer-simulated spectrum (uncoordinated DPPE not included) as described in text. Asterisks indicate impurity.

Table VII. Kinetics of the Thermal Isomerization of *cis*-$Mn(CO)_2(DPPE)_2^+$ from CV Working Curves[a]

temp, °C	v, V s^{-1}	i_c/i_a[b]	log ($k_f\tau$)[c]	k_f, s
0	5	0.46	0.08	19
	10	0.58	−0.16	22
	20	0.72	−0.45	23
	75	0.91	−1.06	21
	100	0.95	−1.26	18
				av 21 ± 2
23	50	0.59	−0.20	115
	100	0.72	−0.45	97
	200	0.83	−0.71	96
				av 103 ± 10

[a] From ref 22. [b] Empirically determined as described in ref 54. [c] From working curve in ref 22; τ in s.

Preparation of $HMn(CO)_2(DPPE)_2$ (I). *trans*-$Mn(CO)_2(DPPE)_2^+Cl^-$[12] (2.0 g, 2.12×10^{-3} mol) was added to 70 mL of THF in a reduction flask equipped with a stopcock on the underside for the ready removal of the excess sodioamalgam. To this solution was added 5 mL of 1% Na (w/w) in Hg, and the solution was stirred magnetically for 2 h, after which the IR spectrum revealed the complete formation of $HMn(CO)_2(DPPE)_2$ (ν_{CO} = 1915, 1856 cm^{-1}) with none of *t*-II remaining (ν_{CO} = 1897 cm^{-1}). Drainage of the excess amalgam, followed by filtration of the cloudy gray solution through a column of Celite (Aldrich) resulted in a clear golden yellow solution. Removal of the THF in vacuo yielded 1.6 g (83%) of the beige $HMn(CO)_2(DPPE)_2$ that was sufficiently pure for the preparation of *cis*-$Mn(CO)_2(DPPE)_2^+AsF_6^-$. Analytically pure material was obtained by recrystallization from a mixture of benzene/hexane at −10 °C. Anal. Calcd for $HMn(CO)_2(DPPE)_2$: C, 71.4; H, 5.43. Found: C, 70.97; H, 5.75.[50] The molecular structure of $HMn(CO)_2(DPPE)_2$ was largely deduced from its ^1H and $^{31}P\{^1H\}$ NMR spectra. The latter consisted of four principal resonances at δ −13.3 (d, 1 P), 71 (m, 1 P), 88 (m, 1 P), and 105 (m, 1 P). The unique high-field doublet resonance at δ −13.3 (J_{PP} = 36.6 Hz) was readily assigned to the pendant, uncoordinated end of an η^1-DPPE ligand by comparison with the NMR spectrum of free

(45) (a) Bond, A. M.; Colton, R.; McDonald, M. E. *Inorg. Chem.* **1978**, *17*, 2842. (b) Bond, A. M.; Grabaric, B. S.; Grabaric, Z. *Inorg. Chem.* **1978**, *17*, 1013. (c) Bond, A. M.; Colton, R.; McCormick, M. J. *Inorg. Chem.* **1977**, *16*, 155. (d) See also ref 3a, 6a, 7, and 19.

(46) (a) Carriedo, G. A.; Riera, V.; Connelly, N. G.; Raven, S. J. *J. Chem. Soc., Dalton Trans.* **1987**, 1769. (b) Connelly, N. G.; Raven, S. J.; Carriedo, G. A.; Riera, V. *J. Chem. Soc., Chem. Commun.* **1986**, 992. (c) Connelly, N. G.; Hassard, K. A.; Orpen, A. G.; Raven, S. J. *J. Chem. Soc., Dalton Trans.* **1988**, 0000. (d) Carriedo, G. A.; Connelly, N. G.; Crespo, M. C.; Quarmby, I. C.; Riera, V. *J. Chem. Soc., Chem. Commun.* **1988**, 0000. (e) For a general review see: Geiger, W. E.; Connelly, N. G. *Adv. Organomet. Chem.* **1984**, *23*, 2. (f) See also Rieke, R. D.; Kojima, H.; Ofele, K. *J. Am. Chem. Soc.* **1976**, *98*, 6735.

(47) Vallat, A.; Person, M.; Roullier, L.; Laviron, E. *Inorg. Chem.* **1987**, *26*, 332.

(48) Vila, J. M.; Shaw, B. L. *J. Chem. Soc., Chem. Commun.* **1987**, 1778.

(49) (a) Kuchynka, D. J.; Amatore, C. A.; Kochi, J. K. *Inorg. Chem.* **1986**, *25*, 4087. (b) Kuchynka, D. J.; Amatore, C. A.; Kochi, J. K. *J. Organomet. Chem.* **1987**, *328*, 133.

(50) Elemental analysis by Atlantic Microlabs, Inc., Atlanta, GA.

Table VIII. Atomic Coordinates (×10⁴) and Equivalent Isotropic Displacement Parameters (10³ Å²) for $Mn(CO)_2(DPPE)_2^+AsF_6^-$

	x	y	z	U(eq)[a]		x	y	z	U(eq)[a]
				cis-$Mn(CO)_2(PPh_2CH_2CH_2PPh_2)_2^+AsF_6^-$					
Mn	2000	4206 (1)	3000	29 (1)	C(29)	4314 (5)	3543 (3)	2814 (3)	44 (2)
As	322 (1)	3047 (1)	5569 (1)	60 (1)	C(30)	4558 (5)	4253 (3)	3059 (3)	47 (3)
P(1)	1141 (2)	4036 (1)	1979 (1)	32 (1)	C(31)	2804 (5)	2456 (3)	2699 (3)	38 (2)
P(2)	886 (2)	5103 (1)	3004 (1)	33 (1)	C(32)	2065 (6)	2065 (3)	2904 (3)	50 (2)
P(3)	3113 (2)	3277 (1)	3066 (1)	34 (1)	C(33)	1839 (6)	1418 (4)	2662 (3)	59 (2)
P(4)	3490 (2)	4820 (1)	2792 (1)	35 (1)	C(34)	2352 (6)	1174 (4)	2198 (3)	63 (2)
F(1)	852 (5)	3408 (3)	4996 (2)	111 (3)	C(35)	3087 (6)	1571 (4)	1990 (3)	54 (2)
F(2)	1492 (4)	2931 (3)	5966 (3)	113 (3)	C(36)	3330 (6)	2216 (4)	2231 (3)	49 (2)
F(3)	−826 (5)	3179 (4)	5171 (3)	148 (4)	C(37)	3547 (5)	2957 (3)	3841 (3)	39 (2)
F(4)	355 (7)	2290 (3)	5259 (3)	140 (4)	C(38)	2921 (6)	2989 (4)	4290 (3)	55 (2)
F(5)	246 (6)	3813 (3)	5894 (3)	130 (3)	C(39)	3231 (6)	2696 (4)	4868 (4)	64 (2)
F(6)	−197 (5)	2681 (3)	6153 (3)	117 (3)	C(40)	4167 (7)	2388 (4)	4972 (4)	64 (2)
O(1)	2664 (4)	4577 (3)	4271 (2)	57 (2)	C(41)	4771 (7)	2353 (4)	4535 (4)	71 (3)
O(2)	407 (4)	3319 (2)	3369 (2)	55 (2)	C(42)	4467 (6)	2631 (4)	3959 (3)	56 (2)
C(1)	2427 (5)	4420 (3)	3771 (3)	36 (2)	C(43)	3675 (5)	5047 (3)	2015 (3)	35 (2)
C(2)	1041 (5)	3668 (3)	3219 (3)	35 (2)	C(44)	2901 (6)	5362 (3)	1655 (3)	44 (2)
C(3)	290 (5)	4762 (3)	1793 (3)	37 (2)	C(45)	2994 (6)	5559 (3)	1055 (3)	51 (2)
C(4)	−120 (5)	5029 (3)	2359 (3)	43 (2)	C(46)	3875 (6)	5443 (4)	837 (4)	65 (2)
C(5)	1726 (5)	3942 (3)	1280 (3)	35 (2)	C(47)	4675 (7)	5143 (4)	1200 (4)	73 (3)
C(6)	1209 (6)	4152 (4)	727 (3)	55 (2)	C(48)	4576 (6)	4945 (4)	1788 (3)	60 (2)
C(7)	1646 (6)	4059 (4)	204 (4)	62 (2)	C(49)	3941 (5)	5593 (3)	3206 (3)	43 (2)
C(8)	2588 (6)	3754 (4)	224 (3)	59 (2)	C(50)	3989 (5)	6208 (3)	2895 (3)	45 (2)
C(9)	3097 (7)	3550 (4)	765 (4)	68 (2)	C(51)	4372 (6)	6781 (4)	3203 (3)	57 (2)
C(10)	2671 (6)	3643 (4)	1302 (3)	53 (2)	C(52)	4727 (6)	6747 (4)	3818 (4)	65 (2)
C(11)	253 (5)	3322 (3)	1864 (3)	38 (2)	C(53)	4689 (6)	6140 (4)	4119 (4)	64 (2)
C(12)	578 (6)	2687 (3)	1695 (3)	50 (2)	C(54)	4309 (6)	5559 (4)	3815 (3)	56 (2)
C(13)	−102 (6)	2147 (4)	1569 (3)	57 (2)	N(1)	7780 (7)	4965 (4)	1047 (4)	131 (4)
C(14)	−1112 (6)	2242 (4)	1604 (3)	58 (2)	C(55)	6765	3886	665	134 (5)
C(15)	−1464 (7)	2851 (4)	1773 (3)	68 (2)	C(56)	7329	4463	886	106 (4)
C(16)	−799 (6)	3400 (4)	1903 (3)	58 (2)	N(2)	1382 (35)	897 (19)	−480 (16)	120
C(17)	107 (5)	5177 (3)	3626 (3)	40 (2)	C(57)	1764	1823	351	120
C(18)	164 (5)	4753 (3)	4125 (3)	45 (2)	C(58)	1555	1334	−113	120
C(19)	−461 (6)	4844 (4)	4570 (3)	60 (2)	N(3)	7203 (23)	4246 (14)	2612 (11)	120
C(20)	−1162 (7)	5368 (4)	4521 (4)	69 (2)	C(59)	7878	3914	3725	120
C(21)	−1234 (7)	5802 (4)	4031 (3)	65 (2)	C(60)	7523	4112	3123	120
C(22)	−621 (6)	5701 (4)	3590 (3)	53 (2)	N(2′)	779 (13)	716 (7)	−294 (6)	120
C(23)	1312 (5)	5992 (3)	2984 (3)	36 (2)	C(57′)	1892	1533	434	120
C(24)	1116 (5)	6392 (3)	2470 (3)	45 (2)	C(58′)	1310	1086	30	120
C(25)	1381 (6)	7062 (4)	2505 (3)	57 (2)	N(3′)	6898 (16)	4071 (9)	2307 (7)	120
C(26)	1831 (7)	7339 (4)	3035 (4)	64 (2)	C(59′)	7573	4309	3439	120
C(27)	2042 (6)	6951 (4)	3556 (3)	56 (2)	C(60′)	7231	4187	2820	120
C(28)	1776 (5)	6262 (3)	3521 (3)	47 (2)					
				trans-$Mn(CO)_2(PPh_2CH_2CH_2PPh_2)^+AsF_6^-$					
Mn(1)	0	5000	5000	32 (1)	C(17)	2690 (8)	817 (7)	5538 (4)	66 (2)
Mn(2)	5000	5000	0	35 (1)	C(18)	3923 (9)	−13 (8)	5820 (4)	82 (3)
As	2221 (1)	1413 (1)	2422 (1)	61 (1)	C(19)	4861 (9)	339 (8)	5913 (4)	84 (3)
P(1)	822 (2)	5221 (2)	3927 (1)	35 (1)	C(20)	4650 (9)	1453 (8)	5726 (4)	85 (3)
P(2)	863 (2)	3053 (2)	4932 (1)	36 (1)	C(21)	3435 (8)	2281 (7)	5421 (4)	66 (2)
P(3)	7178 (2)	4676 (2)	101 (1)	39 (1)	C(22)	−214 (7)	2302 (6)	5130 (3)	44 (2)
P(4)	5416 (2)	5129 (2)	−1160 (1)	41 (1)	C(23)	−1009 (7)	2305 (6)	4622 (4)	62 (2)
F(1)	2361 (6)	559 (5)	3194 (3)	125 (4)	C(24)	−1834 (8)	1713 (7)	4791 (5)	75 (3)
F(2)	3761 (5)	543 (4)	2269 (3)	107 (3)	C(25)	−1836 (8)	1177 (7)	5436 (4)	78 (3)
F(3)	2089 (7)	2296 (5)	1660 (3)	152 (4)	C(26)	−1080 (8)	1157 (7)	5946 (4)	71 (3)
F(4)	698 (5)	2297 (4)	2603 (3)	99 (3)	C(27)	−265 (7)	1735 (6)	5800 (4)	53 (2)
F(5)	1619 (6)	655 (5)	2090 (3)	140 (4)	C(28)	5379 (7)	3473 (7)	161 (3)	44 (4)
F(6)	2838 (5)	2177 (5)	2761 (3)	109 (4)	C(29)	7492 (7)	5498 (6)	−701 (3)	44 (4)
O(1)	2326 (5)	4884 (4)	5714 (3)	55 (3)	C(30)	7039 (7)	5162 (6)	−1291 (3)	48 (4)
O(2)	5580 (5)	2505 (4)	280 (3)	65 (3)	C(31)	7823 (6)	5159 (6)	731 (3)	38 (2)
C(1)	1452 (7)	4908 (6)	5424 (3)	38 (4)	C(32)	7135 (7)	6246 (6)	851 (4)	53 (2)
C(2)	664 (7)	4136 (5)	3538 (3)	42 (4)	C(33)	7585 (8)	6633 (7)	1334 (4)	66 (2)
C(3)	1250 (7)	2958 (6)	4036 (3)	44 (4)	C(34)	8747 (8)	5935 (7)	1691 (4)	60 (2)
C(4)	59 (6)	6529 (6)	3254 (3)	38 (2)	C(35)	9457 (7)	4860 (6)	1584 (4)	54 (2)
C(5)	−1288 (7)	7104 (6)	3191 (3)	46 (2)	C(36)	9003 (7)	4467 (6)	1104 (3)	45 (2)
C(6)	−1915 (8)	8095 (6)	2692 (4)	55 (2)	C(37)	8439 (7)	3215 (6)	147 (3)	41 (2)
C(7)	−1197 (8)	8512 (7)	2244 (4)	71 (3)	C(38)	8369 (7)	2307 (6)	617 (4)	49 (2)
C(8)	141 (9)	7959 (7)	2281 (4)	74 (3)	C(39)	9372 (8)	1194 (7)	696 (4)	71 (3)
C(9)	795 (8)	6951 (6)	2787 (4)	57 (2)	C(40)	10388 (9)	1013 (8)	282 (4)	75 (3)
C(10)	2659 (6)	4907 (6)	3888 (3)	37 (2)	C(41)	10483 (9)	1903 (7)	−196 (4)	80 (3)
C(11)	3446 (7)	4038 (6)	3586 (3)	49 (2)	C(42)	9514 (8)	3012 (7)	−255 (4)	64 (2)
C(12)	4768 (7)	3793 (6)	3605 (4)	57 (2)	C(43)	4327 (6)	6443 (6)	−1747 (3)	40 (2)
C(13)	5227 (8)	4414 (6)	3907 (4)	60 (2)	C(44)	3119 (7)	6559 (7)	−1986 (4)	55 (2)
C(14)	4369 (7)	5298 (6)	4183 (4)	55 (2)	C(45)	2269 (8)	7598 (7)	−2411 (4)	71 (3)
C(15)	3046 (7)	5543 (6)	4182 (3)	44 (2)	C(46)	2622 (8)	8497 (7)	−2585 (4)	69 (3)
C(16)	2411 (6)	1970 (6)	5353 (3)	38 (2)	C(47)	3787 (8)	8417 (7)	−2355 (4)	70 (3)

Table VIII (Continued)

	x	y	z	U(eq)[a]		x	y	z	U(eq)[a]
C(48)	4636 (7)	7395 (6)	−1935 (3)	52 (2)	N	6256	−213	1013	100
C(49)	5626 (7)	3945 (6)	−1579 (4)	48 (2)	C(55)	3796	767	622	100
C(50)	6475 (8)	2847 (7)	−1264 (4)	63 (2)	C(56)	5124	219	851	100
C(51)	6708 (8)	1911 (8)	−1567 (4)	78 (3)	N′	4549	536	−117	100
C(52)	6098 (9)	2092 (8)	−2166 (5)	86 (3)	C(55′)	6134	−249	957	100
C(53)	5244 (9)	3167 (8)	−2491 (5)	93 (3)	C(56′)	5299	183	363	100
C(54)	5023 (8)	4117 (8)	−2195 (4)	73 (3)					

[a] Equivalent isotropic U defined as one-third of the trace of the orthogonalized U_{ij} tensor.

DPPE at δ −13.0 (s). To facilitate the discussion of the spectral assignment of the remaining three phosphorus resonances (Figure 8) the structure is discussed on the basis of the structure below.

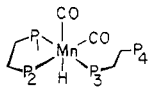

I

Thus the downfield resonances at δ 87.9 (J_{PP} = 36.6, 28.0 Hz) and δ 105.3 (J_{PP} = 28.0, 23.0 Hz) were assigned to the chelated DPPE owing to the large deshielding effect arising from their incorporation into a five-membered ring.[51] Since the trans P–P coupling constant was larger than the cis couplings, P_1 was assigned to the resonances at δ 87.9 and P_2 to δ 105.3, with the former then giving rise to a well-resolved doublet of doublets ($J_{P_1-P_3}$ = 36.6 Hz; $J_{P_1-P_2}$ = 28.0 Hz) and the latter giving an unresolved doublet of doublets ($J_{P_2-P_1}$ = 28.0 Hz; $J_{P_2-P_3}$ = 23.0 Hz). This assignment left P_3 at δ 71.0 as a doublet of triplets ($J_{P_3-P_1}$ = 36.6 Hz; $J_{P_3-P_2}$ = 23.0 Hz; $J_{P_3-P_4}$ = 36.6 Hz). The cis attachment of the hydride was indicated by an upfield resonance centered at δ −7.83 in the ^{1}H NMR spectrum, in which the partially resolved spectrum at 300 MHz was considered to be a doublet of triplets (J_{P-H} = 59 at 41 Hz). Since the magnitudes of the trans P–M–H coupling constants generally cover the range between 70 and 100 Hz,[52] an all cis arrangement of phosphine ligands in a mer configuration shown above was favored. The computer-simulated spectrum in Figure 8 (lower) was constructed with the following parameters: P_4, δ −13.3 (d, $J_{P_4-P_3}$ = 36.6 Hz); P_3, δ 70.0 (dt, $J_{P_4-P_3}$ = 36.6 Hz, $J_{P_3-P_2}$ = 23.0 Hz, $J_{P_3-P_1}$ = 36.6 Hz); P_2, δ 105.3 (dd, $J_{P_2-P_1}$ = 28.0 Hz, $J_{P_2-P_3}$ = 23.0 Hz); P_1, δ 87.9 (dd, $J_{P_1-P_2}$ = 28.0 Hz, $J_{P_1-P_3}$ = 36.6 Hz) (together with the experimental line width of 7 Hz). The hydride abstraction reaction, known to go with stereochemical retention,[14] discussed in the text, further supports the proposed structure.

Preparation of *trans*-Mn(CO)$_2$(DPPE)$_2^+$ Salts. The trans cation *t*-II was prepared as both the bromide and hexafluorophosphate salts according to the methods described in the literature.[11,12] The hexafluoroarsenate salt was prepared for X-ray analysis by the dissolution of *cis*-Mn(CO)$_2$(DPPE)$^+$AsF$_6^-$ in acetonitrile and vapor diffusion of diethyl ether at room temperature in the dark. After 48 h, orange crystals of *trans*-Mn(CO)$_2$(DPPE)$_2^+$AsF$_6^-$ were deposited, and IR analysis showed that the cis to trans isomerization was complete (compare Figure 3).

Preparation of *cis*-Mn(CO)$_2$(DPPE)$_2^+$AsF$_6^-$. The hydridomanganese complex HMn(CO)$_2$(η^2-DPPE)(η^1-DPPE) (I, 1.13 g, 1.25 mmol) from the sodioamalgam reduction of *trans*-Mn(CO)$_2$(DPPE)$_2^+$Br$^-$ in tetrahydrofuran (vide supra) was dissolved in 50 mL of dichloromethane under an argon atmosphere. Upon cooling the solution in an ice bath, $Ph_3C^+AsF_6^-$ (0.65 g, 1.5 mmol) was added portionwise over the course of an hour. During this period, the intensity of the carbonyl bands of I at ν_{CO} = 1856 and 1915 cm^{-1} decreased with the concomitant growth of *c*-II (ν_{CO} = 1894 and 1950 cm^{-1}). When the presence of I was no longer apparent, the volume of the solution was decreased in vacuo at 0 °C. The resulting solution was chromatographed on neutral alumina (Aldrich, activity I) at 0 °C with a 90:10 v/v mixture of acetonitrile/diethyl ether as the eluent. Collection of the fraction consisting of the yellow band was followed by the immediate precipitation of the *c*-II salt with excess, cold ether. This procedure led to 0.75 g (55%) of *cis*-Mn(CO)$_2$(DPPE)$_2^+$AsF$_6^-$ that was free of the trans isomer (IR analysis). The yellow crystals were stored at −10 °C to minimize the slow solid-state isomerization that was noted at room temperature. If the same procedure was followed at room temperature, the IR spectrum of the chromatographic fraction containing the yellow band revealed two carbonyl bands and 1895 and 1953 cm^{-1} with an intensity ratio of ~1.3:1, respectively. Precipitation of the salt from this solution with diethyl ether afforded a light yellow-green powder consisting of *cis*-Mn(CO)$_2$(DPPE)$_2^+$AsF$_6^-$ interlaced with a second microcrystalline orange solid of the trans isomer (ν_{CO} = 1897 cm^{-1}). The isomers could not be fractionally crystallized by using various solvents and cosolvent mixtures. A simpler but inefficient procedure depended on the relative insolubility of *cis*-Mn(CO)$_2$(DPPE)$_2^+$AsF$_6^-$ in tetrahydrofuran. Washing and trituration of the microcrystalline mixture with copious quantities of the THF gradually eroded the orange component and left a small amount of yellow residue of pure cis salt owing to substantial loss of even the less soluble material. Single crystals of *cis*-Mn(CO)$_2$(DPPE)$_2^+$AsF$_6^-$ suitable for X-ray crystallography were grown by the vapor diffusion of diethyl ether into a concentrated acetonitrile solution at 3 °C for 24 h. This temperature was optimum, since there was no evidence of the trans component in the crystalline salt. At lower temperatures, crystal growth led to microcrystalline salt unsuitable for X-ray crystallographic analysis.

Kinetics of the Thermal Isomerization of *cis*-Mn(CO)$_2$(DPPE)$_2^+$. In a typical procedure, *cis*-Mn(CO)$_2$(DPPE)$_2^+$AsF$_6^-$ (0.100 g, 0.091 mmol) was dissolved in 10 mL of dichloromethane under an argon atmosphere. An IR spectrum taken immediately yielded the initial absorbance (A_0) for the carbonyl bands at ν_{CO} = 1894 and 1950 cm^{-1}. The IR spectra were recorded at 30-min intervals for a period of 15 h (~3 half-lives). The steady decrease of the intensity of the carbonyl band at 1950 cm^{-1} was concomitant with what qualitatively appeared to be a steady increase of the intensity of the 1894 cm^{-1} band. The latter arose from the overlapping of the 1897 cm^{-1} band due to trans cation. First-order plots of A_t/A_0 for the 1954 cm^{-1} band was linear with a correlation coefficient of at least 0.99. The same procedure was employed in those kinetics runs containing added DPPE or with 1 atm of carbon monoxide. The rates were also followed by measuring the concentration of *trans*- and *cis*-Mn(CO)$_2$(DPPE)$_2^+$ by their anodic peak currents (i_a). Since the half-wave potential $E_{1/2}$ of these isomers were well-separated (vide supra), the appearance of the *trans* cation *t*-II was easily measured for the kinetics determinations listed in Table IV.

Cyclic Voltammetry of *cis*- and *trans*-Mn(CO)$_2$(DPPE)$_2^+$. In a typical procedure, a thoroughly dried CV cell was filled in an inert-atmosphere box (Vacuum Atmosphere Model MO-41) with a stock solution of THF contraining 0.3 M TBAP. This solution had been exhaustively dried by successively (five times) passing it through a chromatographic column containing anhydrous alumina (Woelm, super 1) that was activated at 450 °C in vacuo at 1 Torr for 12 h. The compartments containing the working electrode and reference arm were similarly filled with anhydrous THF containing 0.3 M TBAP. When prepared this way, the zero-current base line in the CV trace was flat. Under a flow of argon, 0.033 g (3×10^{-5} mol) of *cis*-Mn(CO)$_2$(DPPE)$_2^+$AsF$_6^-$ was added. Initial positive-scan cyclic voltammograms were carried out with a semimicro platinum electrode (radius ~ 0.2 mm) at a variety of scan rates, and most often at 0.5 V s^{-1} unless indicated otherwise. The anodic current was measured and subjected to same kinetics analysis described for the IR method (vide supra).

Kinetics of the Oxidatively Induced Isomerization of *cis*-Mn(CO)$_2$(DPPE)$_2^+$. The oxidatively induced isomerization

(51) Garrou, P. E. *Chem. Rev.* **1981**, *81*, 229.
(52) Saillant, R.; Kaesz, H. D. *Chem. Rev.* **1972**, *72*, 231.

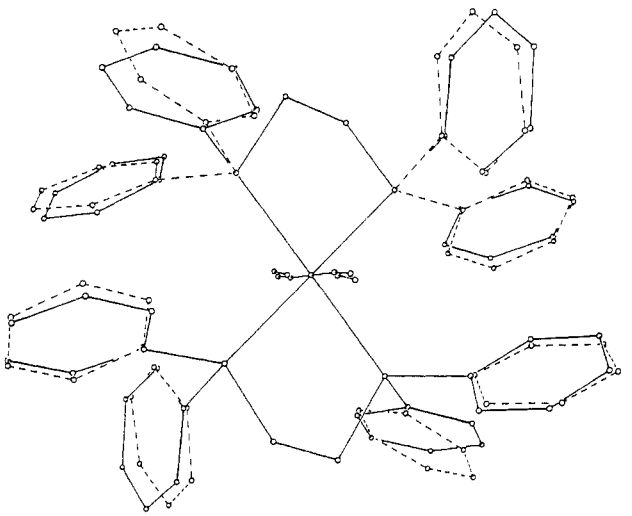

Figure 9. Superposition of the two independent structures of the carbonylmanganese cation in the unit cell of *trans*-$Mn(CO)_2(DPPE)_2^+AsF_6^-$.

of *cis*-$Mn(CO)_2(DPPE)_2^+$ was examined by cyclic voltammetry in acetonitrile rather than tetrahydrofuran to enable faster CV scan rates to be attained in the more polar medium.[27] The cyclic voltammetric studies were carried out with solutions that were 5×10^{-3} M in *c*-I and contained 0.1 M TBAP as supporting electrolyte. Otherwise the procedure described above was used to prepare the solutions of *c*-II for electrolysis. Peak potentials were calibrated with a ferrocene standard with either $E_{1/2} = 0.534$ V vs SCE in THF containing 0.3 M TBAP or $E_{1/2} = 0.406$ V vs SCE in acetonitrile containing 0.1 M TBAP.[53] All voltages were referenced to a saturated calomel electrode with a connection made via an aqueous saturated KCl salt bridge.

The cyclic voltammetric analysis of the oxidatively induced isomerization employed a first-order working curve as described by Nicholson and Shain.[22] This method utilized the current ratio i_c/i_a of *c*-II and *t*-II at various scan rates v. The values of i_c/i_a were obtained empirically by the method described by Nicholson,[54] and in our hands it yielded consistent results (Table VII). The first-order rate constants k_2 were obtained individually from each value of i_c/i_a and the time from the switching potential to $E_{1/2}$ (proportional to v) on the CV trace by comparison with the working curves. The magnitude of k_2 in Table V was the average for v ranging from 5 to 150 V s^{-1} at either 0 or 23 °C, as shown in Table VII.

The digital simulation of the cyclic voltammograms as the kinetics method for the oxidatively induced isomerization of *cis*-$Mn(CO)_2(DPPE)_2^+$ in Scheme I employed Feldberg's method.[23,24] The requisite values of the transfer coefficient α, the heterogeneous rate constant k_s, and the diffusion constants D are listed in Table VI. The mechanism in Scheme I was used to evaluate k_2 by fitting the simulated cyclic voltammograms with the experimental ones until satisfactory currents and current ratios were obtained at all scan rates.[55]

X-ray Crystallography of *cis*- and *trans*-$Mn(CO)_2(DPPE)_2^+AsF_6^-$. A very large yellow square pyramid of *cis*-$Mn(CO)_2(DPPE)_2^+AsF_6^-$ having the approximate dimensions 0.70 × 0.70 × 0.55 mm was mounted in a random orientation on a Nicolet R3m/V automatic diffractometer. Final cell constants, as well as other information pertinent to data collection and refinement, are listed in Table I. The Laue symmetry was determined to be $2/m$, and the space group was shown to be either $C2/c$ or Cc. Intensities were measured by using the Ω scan technique. In reducing the data, Lorentz and polarization corrections were applied, as well as an empirical absorption correction based on ψ scans of 10 reflections having χ values between 70 and 90°. The space group Cc was assumed, and the structure was solved by interpretation of the Patterson map, which revealed the positions of the Mn and As atoms. The remaining non-hydrogen atoms were located in subsequent difference Fourier syntheses. Only the non-phenyl atoms were refined anisotropically. Hydrogens were added at ideal calculated positions and allowed to ride on their respective carbons, with a single variable isotropic thermal parameter. In order to verify that Cc was indeed the correct space group, an analysis of torsion angles in the cation was made. It was found that the two ethano bridges in the DPPE ligands had torsion angles which were opposite in sign, and therefore there could not be a twofold axis passing through Mn and bisecting the carbonyls, as would be required in $C2/c$. After all shift/esd ratios were less than 0.3 (except for the solvent atoms), convergence was reached at the agreement factors listed in Table I. All calculations were made using Nicolet's SHELXTL PLUS (1987) series of crystallographic programs. The final atomic coordinates are included in Table VIII.

A large, bright orange prismatic block of *trans*-$Mn(CO)_2(DPPE)_2^+AsF_6^-$ having approximate dimensions 0.50 × 0.45 × 0.40 mm was coated with a thin layer of quick drying epoxy to prevent solvent loss and treated as described above. The final cell constants pertinent to data collection and refinement, are listed in Table I. The Laue symmetry was determined to be $\bar{1}$, and the space group was shown to be either $P1$ or $P\bar{1}$. Intensities were measured by using the Ω scan technique as described above. The structure was solved by use of the SHELXTL Patterson interpretation program, which revealed the positions of the Mn and As atoms. The asymmetric unit in space group $P\bar{1}$ consisted of two half molecules of the Mn cation, both situated on inversion centers, and one anion in a general position. In order to determine whether there were any significant differences between the two independent cations, a plot was made of the best least-squares fit between the two sets of Mn and P positions. As can be seen in Figure 9, the only noticeable difference between the two structures was in the twisting of some of the phenyl rings, most likely caused by steric packing forces. The positional parameters of the nonhydrogen atoms of *trans*-$Mn(CO)_2(DPPE)_2^+AsF_6^-$ are included in Table VIII.

Preparative-Scale Electrooxidation of *cis*-$Mn(CO)_2(DPPE)_2^+$. A thoroughly dried three-compartment electrolysis cell[49] was charged with anhydrous acetonitrile containing 0.1 M TBAP and 0.33 g (3×10^{-4} mol) of *cis*-$Mn(CO)_2(DPPE)_2^+AsF_6^-$ at 0 °C under an argon atmosphere. The 1×10^{-2} M yellow solution of *c*-II was oxidized at a controlled potential of 1.5 V until the current fell to the background level. At this point the coulometry of the very dark blue-green solution indicated the passage of 28.2 C or 0.97 equiv of charge/mol of *cis*-$Mn(CO)_2(DPPE)_2^+AsF_6^-$ added. IR analysis of the anolyte revealed the presence of a single carbonyl band at ν_{CO} = 1966 cm^{-1} assigned to *trans*-$Mn(CO)_2(DPPE)_2^{2+}$ (*t*-III).[16] Removal of an aliquot of the anolyte for ESR analysis supported this conclusion by a strong spectrum at $\langle g \rangle = 2.000\,14$ showing sextet splitting with $a_{Mn} = 95$ G[7,12] shown in Figure 4. The initial negative-scan cyclic voltammogram of another aliquot of the anolyte revealed the presence of the reversible *t*-III ⇌ *t*-II couple at $E_{1/2} = 0.88$ V, with no other electroactive species apparent.

Acknowledgment. We thank J. D. Korp for crystallographic assistance and the National Science Foundation and R. A. Welch Foundation for financial support.

Registry No. I, 115162-70-4; *c*-II(AsFe)·$3C_2H_3N$, 117872-93-2; *t*-II(AsFe)·C_2H_3N, 117872-95-4; *t*-II(Cl), 14238-89-2; *c*-III, 117956-66-8; *t*-III, 47902-55-6; manganese decacarbonyl, 10170-69-1.

Supplementary Material Available: Tables of observed and calculated structure factors of *cis*-$Mn(CO)_2(DPPE)_2^+AsF_6^-$ and *trans*-$Mn(CO)_2(DPPE)_2^+AsF_6^-$ (35 pages). Ordering information is given on any current masthead page.

(53) Gagne, R. R.; Koval, C. A.; Lisensky, G. C. *Inorg. Chem.* **1980**, *19*, 2854.
(54) Nicholson, R. S. *Anal. Chem.* **1965**, *37*, 1351.
(55) For earlier uses of the method, see: (a) Bockman, T. M.; Kochi, J. K. *J. Am. Chem. Soc.* **1987**, *109*, 7725. (b) See also ref 12 and 13.